THE ASTROPHYSICAL JOURNAL, 283:147–153, 1984 August 1

EXTENDED RADIO OBSERVATIONS OF THE SNR CTB 109

V. A. HUGHES,[1] R. H. HARTEN,[2] C. H. COSTAIN,[3] L. A. NELSON,[1] AND M. R. VINER[1]

Received 1983 September 13; accepted 1984 February 7

ABSTRACT

Observations have been made of the SNR CTB 109 using the Westerbork Synthesis Radio Telescope at λ49 cm and λ21 cm, the Synthesis Telescope of the Dominion Radio Astrophysical Observatory at λ21 cm, and the 46 m telescope of the Algonquin Radio Observatory at λ4.6 cm. The spectral index of the integrated flux density of the SNR is given by $\alpha = 0.50 \pm 0.04$; various maps are compared and show that, over the range of λ4.6–λ49 cm, α does not vary across the SNR. Apart from the fact that the SNR shows an incomplete shell at both X-ray and radio wavelengths, there does not appear to be any correspondence of the finer details in the maps. There is no radio point source near to the position of the X-ray pulsar down to a level of 0.5 mJy at λ21 cm. The SNR appears to consist of a shell with an X-ray pulsar displaced by 3′.6 from the center of curvature, but there is no indication, so far, that the pulsar is associated with the SNR.

Subject headings: interferometry — nebulae: supernova remnants — pulsars — radio sources: general — X-rays: sources

I. INTRODUCTION

The supernova remnant CTB 109 (G109.2−1.0) was discovered as such by Hughes, Harten, and van den Bergh (1981) during a survey of part of the Galactic plane at λ49 cm using the Westerbork Synthesis Radio Telescope (WSRT). It had been detected previously as a nonthermal source by Wilson and Bolton (1960) who designated it CTB 109, by Lynds (1961), and by Raghava Rao *et al.* (1965), but the low brightness, large angular extent of about 36′ × 24′, and its proximity to the strong source Cas A had eliminated it from further study. It was discovered independently as an extended X-ray source by Gregory and Fahlman (1980) using the *Einstein* satellite and was found to contain an X-ray pulsar with a period of 3.4890 s (Fahlman and Gregory 1981). Later observations showed that the period should be twice this, and there was evidence for orbital motion with a period of 2300 s (Fahlman and Gregory 1983).

The original λ49 cm WSRT map, published by Hughes, Harten, and van den Bergh (1981), contains a serious error as described in § II. Since the SNR is of considerable interest because it is only the fourth one known that could have a pulsar associated with it, albeit an X-ray one, we decided to carry out more detailed and extensive mapping using different arrays and independent processing procedures. We have used the Westerbork Synthesis Radio Telescope (WSRT) at λ49 cm and λ21 cm, the Synthesis Telescope of the Dominion Radio Astrophysical Observatory (DRAO) at λ21 cm, and the 46 m paraboloid of the Algonquin Radio Observatory (ARO) at λ4.6 cm. The new WSRT observations have a maximum resolution of 10″ at λ21 cm and 20″ at λ49 cm. The shortest spacings used with the λ49 cm WSRT and the array at DRAO enable the bulk of the angular components to be reproduced, such that some comparison can be made with the λ4.6 cm data which has a resolution of 4′.5.

This paper describes details of the observations, and the results which are shown as a series of maps. There is some discussion on the properties of the SNR.

II. OBSERVATIONS

a) WSRT Observations

The λ49 cm WSRT map published by Hughes, Harten, and van den Bergh (1981), contains an error caused by two factors. First, the size of the object, which is ∼30′, is essentially the size of a 1 × 12 hr grating ring corresponding to the 72 m increment used for the antenna spacing. Second, the observations were done with a minimum spacing of 36 m instead of the usual 72 m, giving spacing numbers in the ratio 1, 3, 5, 7, ... × 36 m. The first grating ring is then primarily negative, but has a broad positive wing and peak on the inside edge before going negative. These two factors caused an artificial shell-like feature to be produced in the southern and western parts of the nebula. If one examines the map carefully, there is some degree of mirror symmetry in the features. Using the CLEAN algorithm on this map only made things worse, since the method could not distinguish between the source and the grating response and tended to redistribute flux into the western part of the shell. The authors were misled since the same features appeared in several observations of fields which overlapped in the region of CTB 109. However, all the observations had been made using a 36 m minimum spacing.

The present WSRT data were obtained during the last quarters of 1980 (λ49 cm) and 1981 (λ21 cm). The observations were centered on CTB 109 (RA 23^h00^m, decl. 58°36′). Because of the earlier difficulties, the new observations were made with complete coverage having spacings every 36 m, such that the grating rings had a radius of ∼40′, which is larger than the size of the object. This required a full 4×12^h synthesis at λ21 cm and a 2×12^h synthesis at λ49 cm. The synthesized beam sizes were 11″ × 13″ and 25″ × 20″ at λ21 cm and λ49 cm, respectively.

Thus, since the grating rings are well outside the object, the

[1] Astronomy Group, Department of Physics, Queen's University at Kingston, Ontario, Canada.
[2] Netherlands Foundation for Radio Astronomy, Dwingeloo, The Netherlands.
[3] Dominion Radio Astrophysical Observatory, Herzberg Institute of Astrophysics, National Research Council of Canada, Penticton, B.C.

new observations do not suffer from the previous problem. As a test, the new 36 m data were processed separately, and we were able to recreate the false western and southern shell features which appeared in the 1981 paper. When the 72 m data were processed separately, the features did not appear. Small residual grating rings from Cas A were present in the λ49 cm map. However, these are located on either side of CTB 109 and do not have any effect on our map.

A different but related problem occurred during the processing of the λ21 cm data. It can be shown that a map obtained from a synthesis observation of a shell or a ring, which has the same size and shape as the grating ring, would be indistinguishable from a point source at the center of the ring. If this map is processed using the CLEAN algorithm, then the point source interpretation will be favored and the shell or ring will be suppressed and treated as a grating ring. An artificial point source did in fact appear at the center of the $2 \times 12^{\rm h}$ maps with the bad grating, even though CTB 109 is not a complete shell or ring, due to the fact that the λ21 cm observations do not contain much flux from the extended component. This was strongest when only half the data ($2 \times 12^{\rm h}$) were processed. It did not appear on the full resolution $4 \times 12^{\rm h}$ map. As a further check on any possible source at the center of the nebula, we made a map using only the longer baseline data, which do not contain any flux from the shell features since they are resolved out. These maps show only the pointlike sources in the field. No point source was found at or near the center of the nebula to a level of 0.5 mJy.

The minimum interferometer spacing at both wavelengths was 36 m. This means that the observations are not sensitive to emission from extended smooth components in the source. At λ49 cm only 25% of the flux from a smooth feature having the size of the nebula would be detected; from extrapolation of the observed visibilities to one at zero spacing, we estimate that our maps at λ49 cm contain only 60% of the total flux of the object. At λ21 cm, the situation is much worse since the shortest spacing, in wavelengths, is much larger and the object is slightly smaller than the primary beam of the antennas. Our observations are essentially insensitive to any components 20′ or larger in size; the WSRT map at λ21 cm contains only ~10% of the total flux in the DRAO map.

The λ21 cm and λ49 cm data were processed using the CLEAN algorithm. The λ49 cm data were cleaned to a level of 5 mJy, resulting in residual antenna and grating response effects being limited to 1 mJy. At λ21 cm the maps were cleaned to a level of 2 mJy, resulting in residual effects of 0.4 mJy or less.

b) *DRAO Observations*

The observations at the DRAO used the Synthesis Telescope (Roger *et al.* 1973) at its normal operating wavelength near λ21 cm. The continuum system receives left-hand circularly polarized radiation in a 15 MHz band centered on the H I line. The line emission is removed by filters. The data set includes 12 hr runs for all spacings which are in units from 4 to 140 times 4.2857 m. The maximum spacing of 2843λ yields a resolution of $1'.0 \times 1'.16$, and the useful field is about 2°.

The data set is dominated at the short spacings by the contribution from the powerful source, Cas A, located 2°.8 to the east. At this separation, the primary grating ring of the Synthesis Telescope passes through the center of the SN field. This contribution was removed from the visibility data by shifting the phase center to solve for the signature of a source at the position of Cas A, with the amplitude and phase as free parameters. This technique worked very well, yielding a smooth run of amplitude and phase corresponding to the known structure of Cas A. These amplitudes and phases were then subtracted from the data to leave only the visibilities of CTB 109. Remaining effects, presumably due to slight changes in the sidelobe pattern and undersampling at the higher spacings, are everywhere less than 1.5% of the peak brightness of CTB 109.

The map has been CLEANed deeply to remove most of the effects of the missing short spacings. When corrected for the remaining zero error (2 mJy per beam) and the primary polar diagram of the 9 m paraboloids, these observations give a total flux for CTB 109 at λ21 cm of 16.8 ± 2 Jy.

c) *ARO Observations*

The ARO Observations were taken at λ4.6 cm using the 46 m telescope of the Algonquin Radio Observatory on 1981 May 17/18 with further observations on 1981 September 23. The cooled parametric amplifier of bandwidth 200 MHz was mounted in the prime focus. The half-power beamwidth for this particular configuaration was 4′.5.

The area mapped was $46' \times 46'$, centered on R.A. $22^{\rm h}59^{\rm m}06^{\rm s}$, decl. 58°36′. The R.A. scans were made at decl. values separated by 0.3 beamwidths. At each decl. value, four scans were made in order to obtain a greater sensitivity to weak emission. Reference scans in declination at two R.A. values were made near the edge of the map in order to tie together the baselines of the main scans. These orthogonal scans were selected at positions where no strong sources were crossed. Using a scan rate of 10 beamwidths per minute and a post-detection bandwidth of 0.25 Hz, the nominal rms noise in the map is ~10 mJy. The positional accuracy of the contours is ~±15″ rms.

In addition, a nearby almost empty region covering the same parallactic angles was mapped in order to check on possible sidelobes due to Cas A. None was found down to a level of ~15 mJy.

III. RESULTS

The results are presented in a series of maps of the SNR, with differing resolving powers and sensitivities. Since the overall size of the SNR is about $36' \times 24'$, various features showed up using the different arrays.

A map obtained at λ21 cm using the WSRT with resolution of 10″ is shown in Figure 1. In this case, the minimum antenna spacing was 36 m so that components of angular size ≥19′ are not included. The lowest contour level is 0.5 mJy. The map was CLEANed, but some grating rings remain. The position of the X-ray pulsar is shown at the coordinate position determined by Gregory and Fahlman (1980), R.A. $22^{\rm h}59^{\rm m}2^{\rm s}.63$, decl. 58°36′37″.6. There is clearly no radio source down to a level of 0.5 mJy within 2′ of the X-ray pulsar. A list of the 20 sources detected, down to a limiting flux density of 0.5 mJy, is shown in Table 1. The total number of expected extragalactic sources within the area of the SNR is 14 ± 4, as estimated from Oosterbaan (1978), which is consistent with the number observed. Thus we can see no evidence for any small diameter radio object at λ21 cm that might be associated with the pulsar.

The λ49 cm WSRT map with the angular resolution of 20″ is shown in Figure 2. Since with this small beam size the

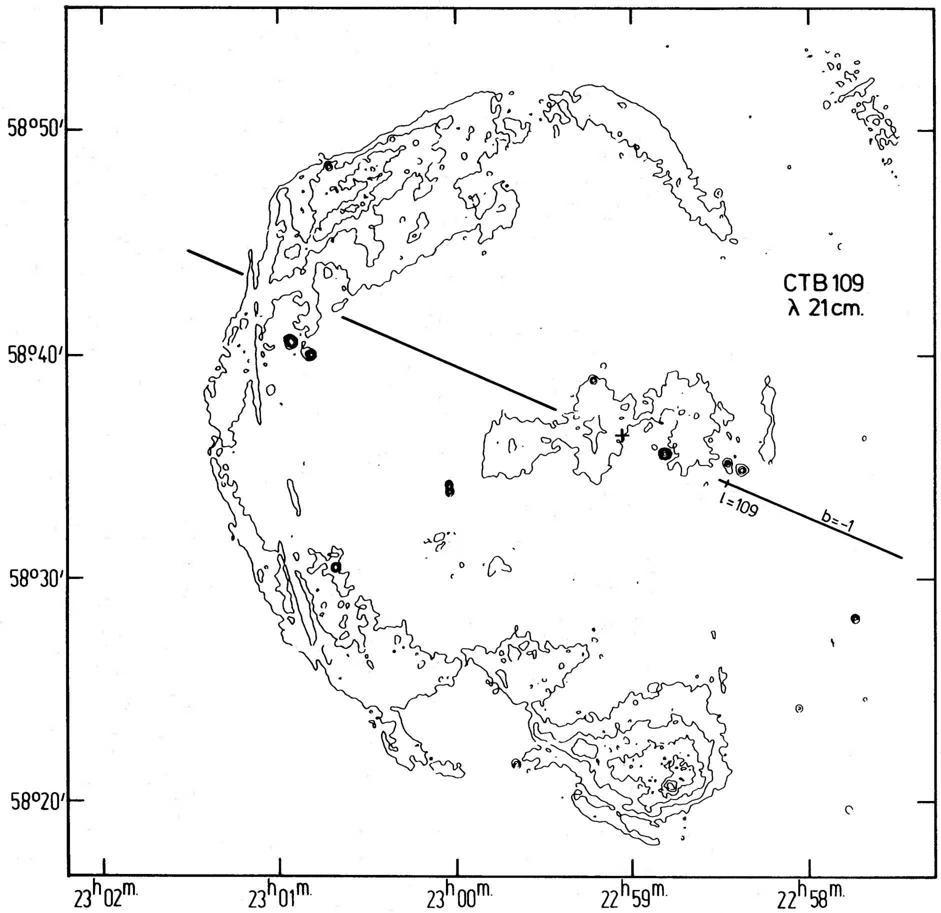

FIG. 1.—Map obtained with the WSRT at λ21 cm designed to show the position of point sources within the area of the SNR. The size of the beam is 10″, and the largest angular component resolved is 19′. Contour units are 0.5–5.5 mJy per beam in steps of 1 mJy per beam, and 10–50 mJy per beam in steps of 10 mJy per beam. The position of the pulsar is shown by a +.

TABLE 1

RADIO SOURCES AT 21 cm IN THE FIELD OF VIEW OF CTB 109

R.A.	Decl.	Flux Density (Jy)
22ʰ57ᵐ52ˢ.2	58°51′16″	0.003
22 58 03.3	58 24 17	0.003
22 58 22.1	58 34 58	0.002
22 58 27.1	58 35 17	0.002
22 58 29.4	58 47 20	0.003
22 58 48.6	58 35 44	0.017
22 58 59.3	58 24 37	0.002
22 59 09.5	58 39 40	0.001
22 59 12.9	58 39 01	0.003
22 59 39.8	58 21 47	0.003
22 59 44.5	58 43 36	0.002
23 00 02.8	58 34 23	0.004 (double)
23 00 12.1	58 26 19	0.002
23 00 22.2	58 49 46	0.003
23 00 41.6	58 30 37	0.006
23 00 43.9	58 48 31	0.004
23 00 46.4	58 48 58	0.003
23 00 49.8	58 40 07	0.005
23 00 57.0	58 40 43	0.011
23 01 03.8	58 38 33	0.001

surface brightness is small, lowest contour levels are at 5 mJy per beam. Various grating rings are evident which are due to adjacent sources, mostly outside the limits of the map. Also evident are several of the discrete sources seen in the higher sensitivity λ21 cm map of Figure 1, most of which, as we have mentioned, are probably extragalactic. We have attempted to obtain the center of curvature of the SNR, and this is shown at R.A. $22^{h}59^{m}.5$, decl. 58°36′.7, together with part of a circle of radius 15′, centered on this point. The transverse separation of the pulsar from the center of curvature is 3′.6, corresponding to a linear separation of 5.2 pc if they are both at the distance that we adopt later of 5 kpc.

Figure 3 shows a comparison of the λ49 cm WSRT map with resolution of 56″ and the DRAO map at λ21 cm with resolution 60″. The contour intervals in each case are in the series 1, 3, 5, 7, ..., but units for the WSRT map are 5 mJy per beam, and those for the DRAO map are 4 mJy per beam. Of note is the remarkable similarity of the two maps, apart from the differences brought about by the presence of suspected extragalactic sources. There is clearly no significant difference in spectral index in the SNR at any point of the maps, including the position of the X-ray source. The variation in spectral index as reported by Sofue, Takahara, and Hirabayashi (1983) is not evident in our data.

The ARO map at λ4.6 cm with resolution of 4′.6 is shown in Figure 4*a*. Clearly evident is the overall low-resolution

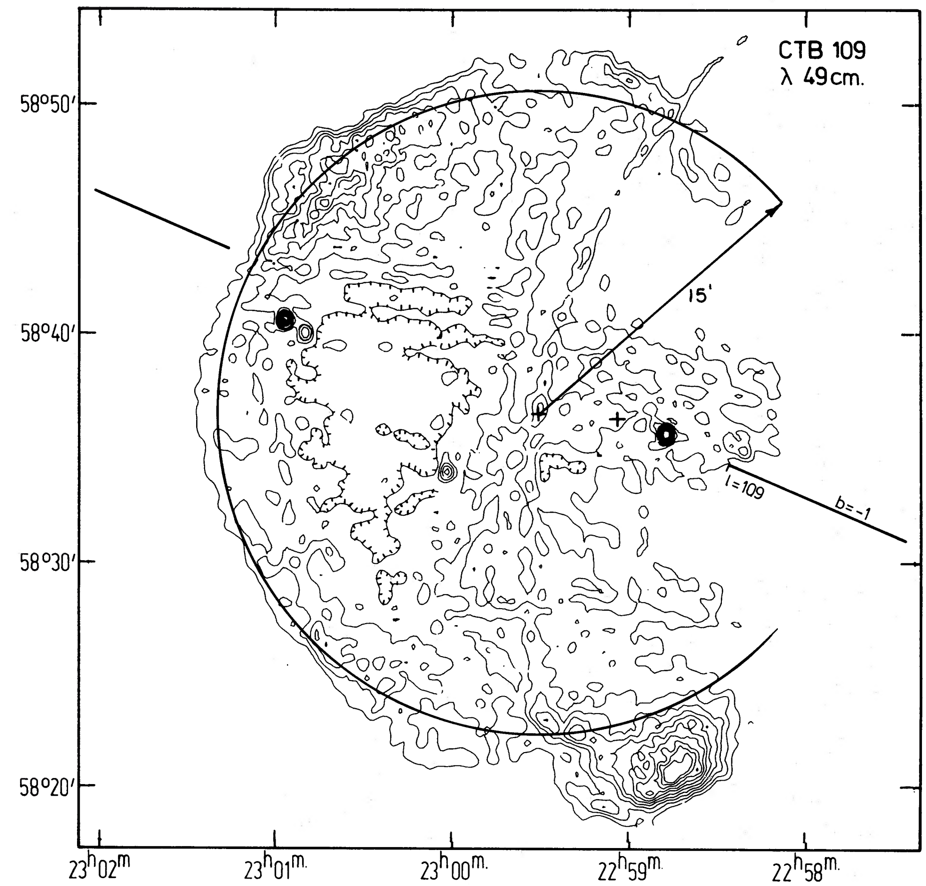

FIG. 2.—Map obtained with the WSRT at λ49 cm and resolution 20″. Largest angular resolution is 47′. Contour levels are 5–50 mJy per beam in steps of 5 mJy per beam. Also shown are the positions of the pulsar and the center of curvature for the arc of a circle 15′ in radius.

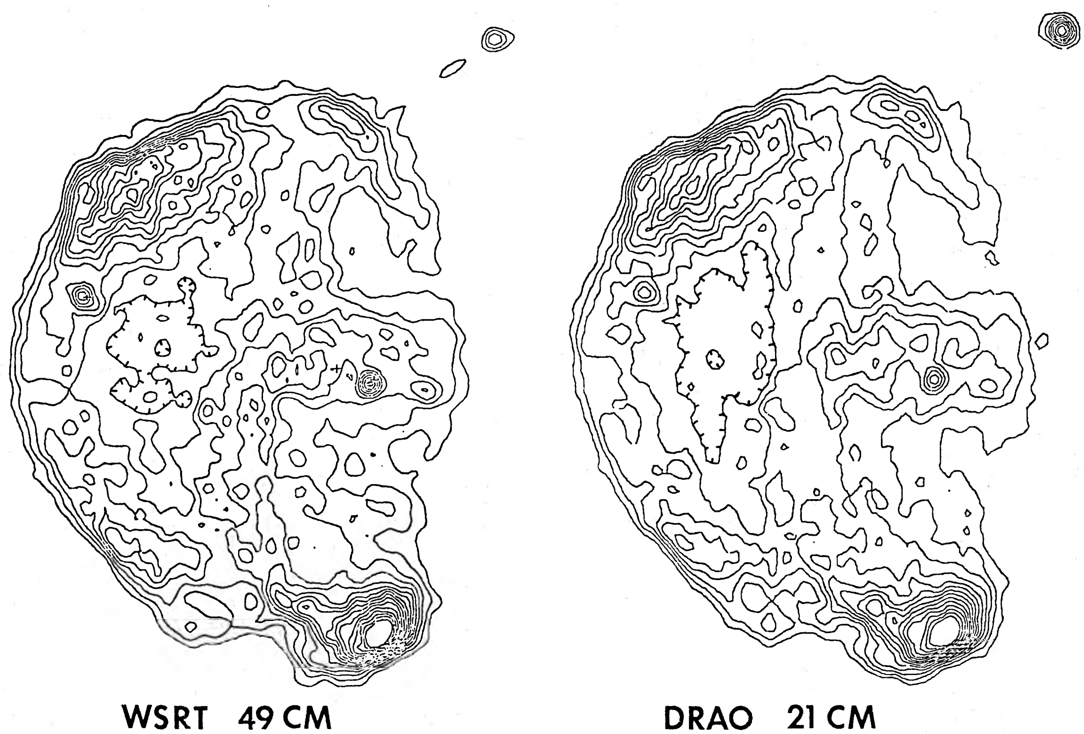

FIG. 3.—Comparison of the WSRT map at λ49 cm and DRAO map at λ21 cm. Resolutions are 56″ and 60″, respectively. Contour intervals are in units of 1, 3, 5, 7, ..., and units for the WSRT map are 5 mJy per beam and for the DRAO map are 4 mJy per beam.

1984ApJ...283..147H

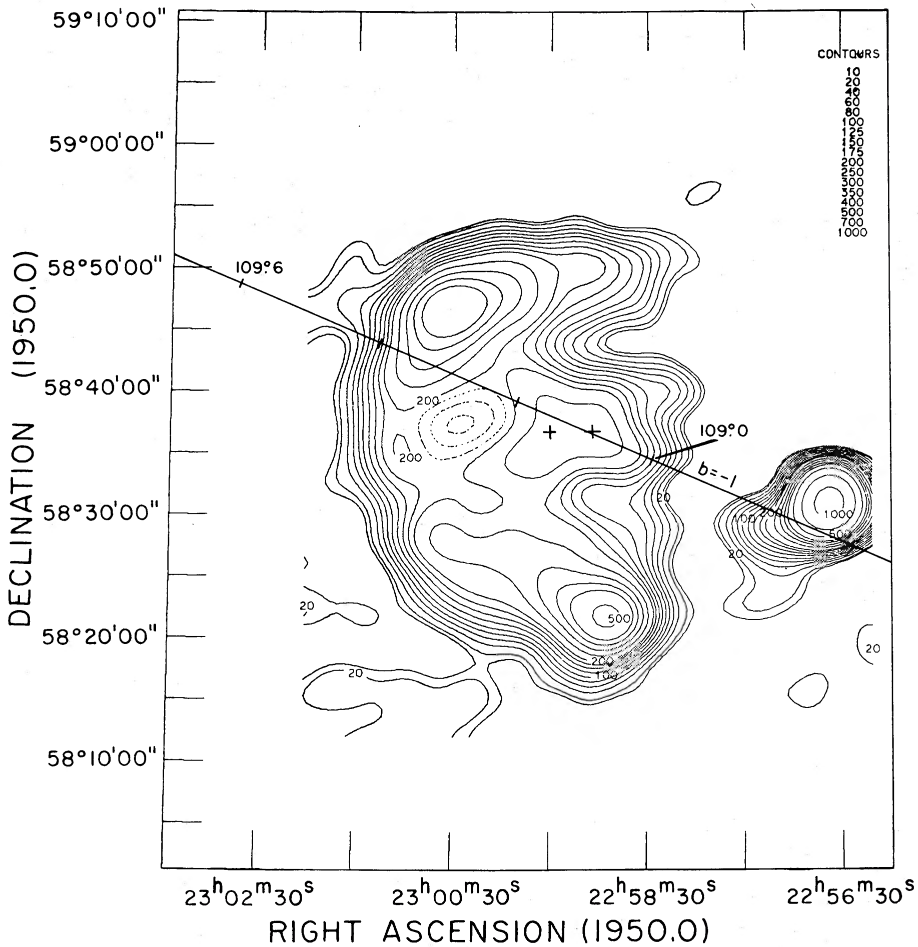

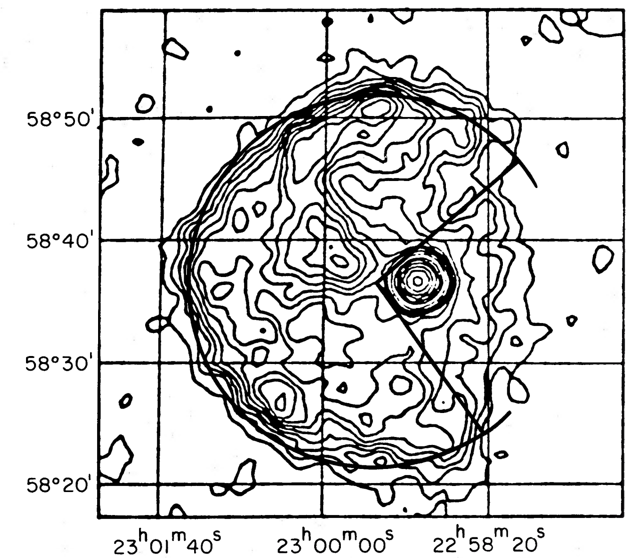

FIG. 4.—(*a*) ARO map at λ4.6 cm and resolution 4'.8. Contour intervals in mJy are shown in the top right-hand corner. (*b*) X-ray map obtained by Gregory and Fahlman (1983) using the IPC detector of the Einstein satellite.

structure of the SNR, the "hole" in the central region with evidence for a ridge to the west of it, the ridge of emission which extends in a northeast direction from the region of more intense emission to the south, and the increased emission to the north. To the west, but separated from the SNR, are the H II regions S152 and S153. Comparison of the DRAO map at λ21 cm convolved with a 4'.8 beam, and the ARO map again shows no significant difference in spectral index anywhere across the SNR. For comparison purposes, the X-ray map obtained by Gregory and Fahlman (1983), which has a resolution of 2'.5 compared with the 4'.6 of the λ4.6 cm map, is also shown in Figure 4*b*.

The flux densities obtained by us, together with those obtained by others, are given in Table 2. The original WSRT estimate of the total flux at λ49 cm was based on a fit to the visibilities and the extrapolated single dish fluxes. The difference between our previous estimate and the present one is due to the fact that in the latter both the UV coverage was improved and the object was centered in the primary beam. Figure 5 shows the spectrum together with the line representing our estimated overall spectral index of $\alpha = 0.50 \pm 0.04$, where we have assumed that the flux density is given by $S \propto \nu^{-\alpha}$, where ν is the frequency.

IV. ANALYSIS OF DATA

a) *Distance*

There are few reliable ways of estimating the distance to the SNR, in particular since there are no known features that can be identified. The method used here is based on an empirical relationship between the brightness (Σ) and diameter (D) obtained for some SNR's whose distances are presumed known. We have used the relationship determined by Caswell and Lerche (1979), but converted to expected flux density (S) at λ73.5 cm (408 MHz) versus distance (d) in kpc, assuming an elliptical source with axes $31' \times 24'$. We obtain:

$$S = 9.82 \times 10^3 d^{-3} \exp(-17.45d/175)\ \mathrm{Jy}\ .$$

From Figure 5, the estimated flux density at λ73.5 cm is 32 Jy, which gives a distance of 5.6 kpc. However due to the very large uncertainties inherent in this method, the estimated error in distance could be at least 30%. Since in the direction of the SNR the Perseus arm appears to bifurcate, the outer section being at a distance of about 5 kpc, we would suggest that the SNR is associated with this outer part of the arm.

TABLE 2

THE SPECTRUM OF CTB 109

Wavelength (cm)	Frequency (GHz)	Flux Density (Jy)	Telescope	Reference
74	0.408	37 ± 6	Bologna Interferometer	1
49	0.610	26 ± 3	WSRT	2
21	1.4	16.8 ± 2	WSRT DRAO	2
11.1	2.7	13 ± 1.5	Bonn 100 m	3
4.6	6.5	6.7 ± 1.0	ARO 46 m	2
3.0	10.2	7.0 ± 0.7	NRO 45 m	4

REFERENCES.—(1) Felli *et al.* 1977. (2) This paper. (3) Downes 1983. (4) Sofue, Takahara, and Hirabayashi 1983.

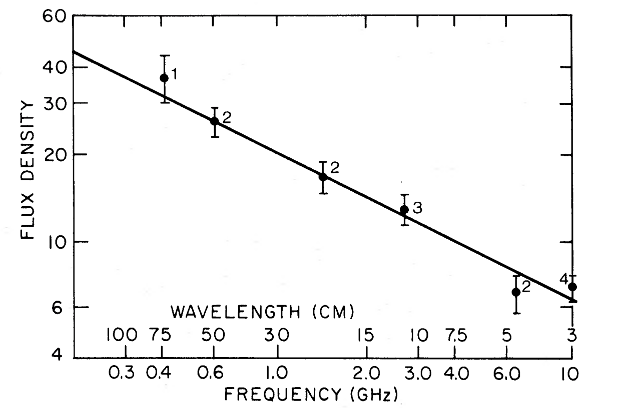

FIG. 5.—Spectrum of CTB 109. The straight line is for a spectral index of $\alpha = 0.50$. Numbers associated with the plotted points are references: 1. Felli *et al.* (1977); 2. This paper; 3. Downes (1982); 4. Sofue *et al.* (1983).

b) *Comparison with the Optical Photograph*

We compared the radio maps with the photograph of the region obtained in the light of [S II] using the Palomar 1.2 m Schmidt telescope (Hughes, Harten, and van den Bergh 1983). As with the previous comparison, we found no fit between the optical filaments and the radio features; we again conclude that the filaments are due to unstable cooling in the region of the shock front where there is a separation between magnetic field and relativistic particles.

c) *Comparison with X-Ray Map*

For comparison with the radio maps, we have reproduced as Figure 4*b* the X-ray map of the SNR obtained by Gregory and Fahlman (1980) using the *Einstein* IPC detector.

There is an overall global agreement in size and shape between the radio and X-ray data, both showing a well-defined shell of the same approximate radius to the east, and incomplete structure to the west. In addition, both have an east-west ridge of emission near their centers. But if we try to compare the two in detail we find few equivalent features. Both have bright spots around the rim as would be expected from the increased optical depth there and the presence of regions of increased emission on the surface of the shell, but these features do not appear to correlate well in detail. In fact, the X-ray map has a ridge of emission that extends across a hole in the radio map.

We have already shown that the X-ray pulsar is not a radio source down to a radio flux density of 0.5 mJy. However, the pulsar appears to be displaced by 3'.6 from the center of curvature of the high-resolution map, and by about the same amount from the center of curvature of the X-ray map, in contradiction to the statement by Gregory and Fahlman (1980). We would point out that 3'.6 is approximately the value of the displacement arrived at by Sofue, Takahara, and Hirabayashi (1983).

V. DISCUSSION

The comparison between radio and X-ray maps have shown that though the global structure is similar at both wavelengths, there is lack of correlation of detailed features. This is as expected if most of the radiation originates in the shell, since the mechanism for radiation at X-ray wavelengths is thermal bremsstrahlung from the hot plasma behind the shock, while at radio wavelengths it is synchrotron emission from relativistic particles in the swept-up magnetic field. In fact, radio emission probably originates from cooled compressed filaments within the hotter X-ray gas (Duin and van der Laan 1975; Dickel and Willis 1980). Since there is no reason why the temperature of the plasma should be simply related to the production of relativistic particles and to the value of the magnetic field, there is no reason for the emissivity at X-ray wavelengths to be linearly related to that at radio wavelengths. The additional fact that there is no measurable variation in the radio spectral index across the source leads to the conclusion that there is no compact radio object or "plerion" at the center. We conclude that most of the radiation is produced in the shell and classify the SNR as a shell type containing an X-ray pulsar within its boundary on the plane of the sky. As far as we know, there is no evidence for radio or γ-ray pulsations.

Of additional interest is the fact that CTB 109, obviously seen in projection, does not exhibit a complete shell. One explanation is the presence of a gradient in the interstellar density, such that one part of the shell shows stronger emission as the result of the shock meeting a higher surrounding density, with a much less well-defined shell on the other side (e.g., Shaver 1982). This property is not unique, being common to a number of other remnants. Gregory *et al.* (1983) suggest that the shock wave is expanding into a molecular cloud where it is absorbed. However, we find this difficult to accept since we would expect just the reverse for the reason stated above.

One additional point may be of significance, namely that the pulsar is displaced from the center of curvature of the SNR by 3′.6 or 5.2 pc for the accepted distance of 5 kpc. If we assume that the pulsar is a remnant of the SN and was at the center of curvature at the time of the explosion, and that the age of the SNR is 1.5×10^4 yr (Hughes, Harten, and van den Bergh 1981; Sofue, Takahara, and Hirabayashi 1983), then the pulsar would have needed an average speed of 340 km s^{-1}, which is less than the maximum transverse speed for pulsars of 400 km s^{-1} as measured by Lyne, Anderson, and Salter (1982). It is possible that the pulsar could acquire this velocity as a consequence of the conservation of momentum during a nonisotropic explosion, since a few solar masses are normally ejected at a speed of 10,000 km s^{-1}, and hence only a slight asymmetry would be needed. Nonisotropic collapse onto a compact object could also give the necessary recoil velocity (e.g., Harrison and Tademaru 1975). Such suggestions, though of interest, are at present highly speculative.

VI. CONCLUSIONS

The SNR CTB 109 has been mapped at λ49 cm, λ21 cm, and λ4.6 cm using three independent sets of observations. The resulting maps show an incomplete shell with no measurable difference in spectral index at any point. If we include with our data those obtained by others, the spectral index of the integrated emission from the whole remnant is $\alpha = 0.50 \pm 0.04$. Comparing our maps with the X-ray data, we see the same overall global features, but no detailed correlation between radio and X-ray features; there is no radio source at the position of the X-ray pulsar with flux density >0.5 mJy at λ21 cm. We conclude that the SNR consists of a shell with no evidence for a filled center, but it does contain, as seen in projection, an X-ray pulsar which is displaced from the center of curvature by 3′.6. If the pulsar is a remnant of the SN, then it is the fourth case of a SNR which contains a pulsar, but the first case in which pulses have not yet been detected at other than X-ray wavelengths. On the other hand, the present data shows no evidence that the association of X-ray pulsar and SNR is other than a chance superposition.

The authors wish to thank Drs. J. L. Caswell and J. R. Dickel for some very useful discussions. The Westerbork Synthesis Radio Telescope is operated by the Netherlands Foundation for Radio Astronomy (SRZM) with financial support of the Netherlands Organization for the Advancement of Pure Research (ZWO). The Dominion Radio Astrophysical Observatory and the Algonquin Radio Observatory are operated by the Herzberg Institute of Astrophysics of the National Research Council of Canada. Some of the work was supported by an Operating Grant from the Natural Sciences and Engineering Research Council (NSERC) of Canada. L. A. N. wishes to acknowledge the award of an NSERC Scholarship.

REFERENCES

Caswell, J. L., and Lerche, I. 1979, *M.N.R.A.S.*, **187**, 201.
Dickel, J. R., and Willis, A. G. 1980, *Astr. Ap.*, **85**, 55.
Downes, A. 1983, *M.N.R.A.S.*, **203**, 695.
Duin, R. M., and van der Laan, H. 1975, *Astr. Ap.*, **40**, 111.
Fahlman, G. G., and Gregory, P. C. 1981, *Nature*, **293**, 202.
———. 1983, in *IAU Symposium 101, Supernova Remnants and Their X-ray Emission*, ed. P. Gorenstein and J. Danziger (Dordrecht: Reidel), p. 445.
Felli, M., Tofani, G., Fanti, C., and Tomasi, P. 1977, *Astr. Ap. Suppl.*, **27**, 181.
Gregory, P. C., Braun, R., Fahlman, G. G., and Gull, S. F. 1983, in *IAU Symposium 101, Supernova Remnants and Their X-ray Emission*, ed. P. Gorenstein and J. Danziger (Dordrecht: Reidel), p. 437.
Gregory, P. C., and Fahlman, G. G. 1980, *Nature*, **287**, 805.
———. 1983, in *IAU Symposium 101, Supernova Remnants and Their X-ray Emission*, ed. P. Gorenstein and J. Danziger (Dordrecht: Reidel), p. 429.
Harrison, E. R., and Tademaru, E. 1975, *Ap. J.*, **201**, 447.
Hughes, V. A., Harten, R. H., and van den Bergh, S. 1981, *Ap. J. (Letters)*, **246**, L127.
Lynds, C. R. 1961, *Pub. N.R.A.O.*, **1**, 43.
Lyne, A. G., Anderson, B., and Salter, M. J. 1982, *M.N.R.A.S.*, **201**, 503.
Oosterbaan, C. E. 1978, *Astr. Ap.*, **69**, 235.
Raghava Rao, R., Medd, W. J., Higgs, L. A., and Broten, N. W. 1965, *M.N.R.A.S.*, **129**, 159.
Roger, R. S., Costain, C. H., Lacey, J. D., Landecker, T. L., and Bowers, F. K. 1973, *Proc. IEEE*, **61**, 1270.
Shaver, P. A. 1982, *Astr. Ap.*, **105**, 306.
Sofue, Y., Takahara, F., and Hirabayashi, H. 1983, *Pub. Astr. Soc. Japan*, **35**, 447.
Wilson, R. W., and Bolton, J. G. 1960, *Pub. A.S.P.*, **72**, 331.

C. H. Costain: Dominion Radio Astrophysical Observatory, Herzberg Institute of Astrophysics, National Research Council of Canada, Box 248, Penticton, B.C. V2A 6K3, Canada.

R. H. Harten: Netherlands Foundation for Radio Astronomy, Radiosterrenwacht, Postbus 2, 7990 AA Dwingeloo, The Netherlands.

V. A. Hughes, L. A. Nelson, and M. R. Viner: Astronomy Group, Department of Physics, Queen's University, Kingston, Ontario K7L 3N6, Canada.